An Analytical Study of Heat and Mass Transfer in Multiparticle Systems at Low Reynolds Numbers

ROBERT PFEFFER and JOHN HAPPEL
New York University, New York, New York

This investigation was undertaken to obtain an analytical solution to the problem of predicting particle-to-fluid heat and mass transfer rates in multiparticle systems at low Reynolds numbers. The energy equation based on the free surface model was solved by expanding the fluid temperature distribution in even powers of the spherical angle and by assuming that the fluid properties remain relatively constant with temperature. Solutions were obtained for Peclet numbers between 0.1 and 100 and fractional void volumes between 0.4 and 1.0. They show that the average Nusselt or Sherwood number in a bed of particles is a function of both the fractional void volume and the Peclet number, the effect of Peclet number decreasing as the bed becomes more concentrated in the low Peclet number range. A plot of the results in terms of the *j* factor vs. the Reynolds number shows good agreement with published experimental mass and heat transfer data and indicates that the *j* factor is not independent of the Schmidt or Prandtl numbers at low Reynolds number, low Peclet number flow.

The problem of predicting particle-to-fluid heat and mass transfer rates is widely encountered in the chemical process industries. Examples include fixed or moving bed pebble heaters, heat recovery operations in which a granular catalyst is cooled by direct contact with a flowing fluid, drying of a gas by a granular absorbent, regeneration of a used absorbent, sublimation of solid particles into a gaseous stream, solution of solid particles into a liquid stream, roasting of ores, catalytic chemical reactions, and numerous other applications. It is therefore not surprising that a large number of experimental particle-to-fluid heat and mass transfer correlations have been reported in the recent literature. However most of these correlations do not agree too well with each other, especially in the low Reynolds number range, and since almost all of the data were reported in the void fraction range $\epsilon = 0.4$ to $\epsilon = 0.6$, the effect of void volume on heat and mass transfer rates is not well established. The purpose of the investigation described in this paper was to obtain a theoretical solution to the problem which would complement the experimental results in the low Reynolds number range as well as indicate the effect of voidage and other pertinent variables.

FREE SURFACE MODEL FOR HEAT OR MASS TRANSPORT

The free surface model used successfully by Happel (*11, 12*) in his study of the rate of sedimentation and pressure drop in packed beds and flow relative to arrays of cylinders was applied to the present study. The model is developed on the basis that two concentric spheres will describe a typical cell in a random assemblage which is considered to consist of many cells, each of which contains a particle surrounded by a fluid envelope. Each cell contains the same amount of fluid as the relative volume of fluid to particle volume in the entire assemblage. In an actual packed bed these fluid envelopes will be distorted, but it is assumed that a typical cell can be taken to be spherical. Also the outside surface of each cell is assumed to be frictionless or having a free surface. Thus the entire disturbance due to each particle is confined to the cell of fluid with which it is associated. For the case of heat or mass transport the temperature or concentration of the forward moving fluid is assumed to be that of the cell boundary.

Consider a solid sphere of radius a placed at the origin of an r, θ, ϕ spherical coordinate system surrounded by a spherical envelope of fluid having a free surface at radius b. If one assumes that the fluid envelope moves past the solid sphere whose temperature is constant with a constant velocity V, and that one has a steady state, then an energy balance around a differential element of fluid yields

$$\alpha\left(\frac{\partial^2 t}{\partial r^2} + \frac{2}{r}\frac{\partial t}{\partial r} + \frac{1}{r^2 \sin\theta}\frac{\partial}{\partial \theta}\right)\left(\sin\sigma\frac{\partial t}{\partial \theta}\right) - \left(v_r\frac{\partial t}{\partial r} + \frac{v_\theta}{r}\frac{\partial t}{\partial \theta}\right) = 0 \quad (1)$$

Since flow at low Reynolds numbers is being considered, a solution is chosen to the creeping motion equations to obtain the fluid velocity components v_r and v_θ. Happel (*11*), using spherical harmonics, gives a solution to these equations for the case of a sphere falling in the fluid contained in a concentric sphere:

$$v_r = \left(-2C - 2Dr^2 - \frac{2A}{r^3} - \frac{2B}{r}\right)\cos\theta \quad (2)$$

$$v_\theta = \left(-A/r^3 + \frac{B}{r} + 2C + 4Dr^2\right)\sin\theta \quad (3)$$

The unknown constants A, B, C, and D are evaluated

Robert Pfeffer is at the City College of the City University of New York, New York, New York.

from the boundary conditions specified by the free surface model which are

$$v_x = V, v_y = v_z = 0 \quad at\ r = a \qquad (4)$$

$$v_r = 0$$

$$\tau_{r\theta} = \mu \left(\frac{\partial v_r}{r\partial\theta} + \frac{\partial v_\theta}{\partial r} - \frac{v_\theta}{r} \right) = 0 \quad \text{at } r = b \qquad (5)$$

Application of these boundary conditions to Equations (2) and (3) gives

$$A = \frac{a^3 V}{2w}, B = \frac{-a V (3 + 2\gamma^5)}{2w}, C = \frac{V (3 + 2\gamma^5)}{2w}$$

$$D = \frac{-V \gamma^5}{2 a^2 w} \qquad (6)$$

where $\gamma = a/b$, and $w = 2 - 3\gamma + 3\gamma^5 - 2\gamma^6$.

To obtain the velocity components v_r and $v\theta$ on the basis that the inner sphere is stationary and that the fluid envelope is moving with the velocity V, one simply needs to add $- V \cos \theta$ to v_r and $+ V \sin \theta$ to v_θ in Equations (2) and (3).

Method of Solution

If

$$\rho = \frac{r}{a} \text{ and } \psi = \frac{T_1 - t}{T_1 - T_0}$$

where T_1 is the temperature of the inner sphere at $r = a$ and T_0 is the temperature of the fluid envelope at $r = b$, then Equation (1) can be written in terms of dimensionless quantities

$$\frac{\partial^2\psi}{\partial\rho^2} + \frac{2}{\rho}\frac{\partial\psi}{\partial\rho} + \frac{1}{\rho^2}\left(\frac{\partial^2\psi}{\partial\theta^2} + \cot\theta\frac{\partial\psi}{\partial\theta} \right) = \frac{a}{\alpha}\left(v_r\frac{\partial\psi}{\partial\rho} + \frac{v_\theta}{\rho}\frac{\partial\psi}{\partial\theta} \right) \qquad (1a)$$

Therefore the boundary value problem consistent with the free surface model involves solving Equation (1*a*) subject to the boundary conditions

$$\left.\begin{array}{l} \rho = 1, \psi = 0 \\ \rho = b/a, \psi = 1 \end{array}\right\}$$

Equation (1*a*), although linear, cannot be solved in closed form and must be approximated by some sort of perturbation procedure. Solutions based on expanding the quantity ψ in terms of a power series in N_{Pe} were attempted by Kronig and Bruijsten (*14*) and by Frisch (7) in their study of heat and mass transfer from a single sphere into a Stokes velocity field. This classical approach however fails to satisfy all of the boundary conditions and hence was found unsuitable. An alternative solution suggested by Yuge (*24*) in his study of the same problem involved expanding the quantity ψ in an even power series of the spherical angle θ with coefficients that are functions of ρ alone, for example

$$\psi = f_0(\rho) + f_2(\rho)\,\theta^2 + f_4(\rho)\,\theta^4 + \ldots\ldots \qquad (7)$$

This type of an expansion, although it cannot be proven to be mathematically rigorous, seems logical since in the limiting case, as the Reynolds number approaches zero, the temperature distribution will be the same as that for a sphere in a stationary medium (if natural convection is neglected) and hence independent of the angle θ. It also does not limit us to Peclet numbers less than 1.0.

Using the Yuge approach one neglects the term

$$\frac{1}{\rho^2}\left(\frac{\partial^2\psi}{\partial\theta^2} + \cot\theta\frac{\partial\psi}{\partial\theta} \right)$$

in Equation (1*a*), so that as a first approximation

$$\frac{\partial^2\psi}{\partial\rho^2} + \frac{2}{\rho}\frac{\partial\psi}{\partial\rho} = \frac{a}{\alpha}\left(v_r\frac{\partial\psi}{\partial\rho} + v_\theta\frac{\partial\psi}{\partial\theta} \right) \qquad (1b)$$

If Equation (7) is substituted into Equation (1*b*) and the fluid velocity components v_r and v_θ given by the free surface model are used, one obtains

$$-\frac{N_{Pe} \times M}{2}[\cos\theta\, f_0'(\rho) + \cos\theta\, f_2'(\rho)\,\theta^2 + \cos\theta\, f_4'(\rho)\theta^4] + \frac{N_{Pe} \times N}{2\,\rho}[2\,f_2(\rho)\theta\sin\theta + 4\,f_4(\rho)\theta^3\sin\theta] - f_0''(\rho) - f_2''(\rho)\theta^2 - f_4''(\rho)\theta^4 - \frac{2\,f_0'(\rho)}{\rho} - \frac{2\,f_2'(\rho)\theta^2}{\rho} - \frac{2\,f_4'(\rho)\theta^4}{\rho} + \text{higher order terms} = 0 \qquad (8)$$

where

$$M = \frac{-v_r}{V\cos\theta}, N = \frac{v_\theta}{V\sin\theta}, \text{ and } N_{Pe} = \frac{2aV}{\alpha}$$

One now expands $\cos\theta$ and $\sin\theta$ in powers of θ, and equating powers of θ in Equation (8) obtains an infinite set of linear, second order total differential equations, the first three of which are

$$f_0''(\rho) + \left(\frac{2}{\rho} + \frac{N_{Pe} \times M}{2}\right) f_0'(\rho) = 0 \qquad (9)$$

$$f_2''(\rho) + \left(\frac{2}{\rho} + \frac{N_{Pe} \times M}{2}\right) f_2'(\rho) - \frac{N_{Pe} \times N}{\rho} f_2(\rho) = \frac{N_{Pe} \times N}{4} f_0'(\rho) \qquad (10)$$

$$f_4''(\rho) + \left(\frac{2}{\rho} + \frac{N_{Pe} \times M}{2}\right) f_4'(\rho) - \frac{2\,N_{Pe} \times M}{\rho} f_4(\rho) = \frac{N_{Pe} \times M}{2}\left(\frac{f_2'(\rho)}{2!} - \frac{f_0'(\rho)}{4!}\right) - \frac{N_{Pe} \times N}{\rho}\,\frac{f_2(\rho)}{3!} \qquad (11)$$

The equations are subject to the boundary conditions

$$f_0(\rho) = f_2(\rho) = f_4(\rho) = \ldots. = 0 \text{ at } \rho = 1$$

$$f_0(\rho) = 1, f_2(\rho) = f_4(\rho) = \ldots. = 0 \text{ at } \rho = \frac{b}{a} = \frac{1}{\gamma}$$

Yuge (*24*) has solved these equations numerically for the problem of heat transfer to a sphere in a Stokes' velocity field and found that not only did solutions exist for all of the equations which he solved, but that the convergence of the coefficients f_0, f_2, f_4, etc. was extremely rapid.

The second approximation is obtained by letting

$$\psi = g_0(\rho) + g_2(\rho)\theta^2 + g_4(\rho)\theta^4 + \ldots. \qquad (12)$$

and substituting the first approximation [Equation (7)] back into the term that was omitted in Equation (1*b*). Using the same procedure as before one obtains a second infinite set of linear, second order differential equations, the first three of which are

$$g_0'' + \left(\frac{N_{Pe} \times M}{2} + \frac{2}{\rho}\right) g_0' = -\frac{4f_2}{\rho^2} \qquad (9a)$$

$$g_2'' + \left(\frac{N_{Pe} \times M}{2} + \frac{2}{\rho}\right) g_0' - \frac{N_{Pe} \times N}{\rho} g_2 = \frac{N_{Pe} \times M}{4} g_0' + \left[\frac{16\,f_4 - \frac{2\,f_2}{3}}{2}\right] \qquad (10a)$$

$$g_4'' + \left(\frac{N_{Pe} \times M}{2} + \frac{2}{\rho}\right) g_4' - \frac{2\,N_{Pe} \times N}{\rho} g_4 - \frac{N_{Pe} \times M}{2}$$

$$\left(\frac{g_2'}{2!}-\frac{g_0'}{4!}\right)-\frac{N_{Pe}\times N}{\rho}\frac{g_2}{3!}-\frac{4f_4}{3}-\frac{2f_2}{45} \quad (11a)$$

Succeeding approximations can be obtained in a similar manner.

In the present paper the Yuge procedure was used to obtain an approximate solution to the energy Equation (1*a*) coupled with the free surface model. Numerical solutions of Equations (9), (10), (11), (9*a*), and (10*a*) were computed with the Runge-Kutta initial-value procedure with Gill's coefficients for Peclet numbers between 0.1 and 100 for different values of γ. Since boundary conditions rather than initial conditions were specified, an iterative procedure which involved guessing the unknown initial condition and then matching the boundary condition was necessary. All of the numerical work was done on a high-speed digital computer.

Heat and Mass Transfer Rates

If h is the coefficient of heat transfer at the surface of the inner sphere of the model, or more generally the heat transfer coefficient at the surface of a particle in a packed bed, then a heat balance yields

$$h=\frac{-k\left(\frac{\partial t}{\partial r}\right)_{r=a}}{T_1-T_0} \quad (13)$$

$T_1 - T_0$ is the temperature difference between the particle and the cell boundary. For the limiting case of very slow flow through an idealized bed the flow from one cell to another can be taken to be at the temperature of the outside boundary of each cell, since the fluid temperature changes very slowly as it passes from one cell to another.

If the second approximation [Equation (12)] is used to represent the fluid temperature distribution, Equation (13) can be written in terms of the dimensionless local Nusselt number as

$$N_{Nu} = 2[g_0'(\rho) + g_2'(\rho)\theta^2 + g_4'(\rho)\theta^4]_{\rho=1} \quad (14)$$

The average Nusselt number around the particle is evaluated by integrating the local Nusselt number over the surface of the sphere so that

$$(N_{Nu})_{avg} = \frac{1}{4a^2}\int_0^{\pi} Nu \cdot 2a^2 \sin\theta\, d\theta \quad (15)$$

or

$$(N_{Nu})_{avg} = [2\, g_0'(\rho) + 5.87\, g_2'(\rho) + 26.97\, g_4'(\rho)]_{\rho=1}$$

Values of $f_0'(\rho)$, $f_2'(\rho)$, $f_4'(\rho)$, $g_0'(\rho)$, etc. evaluated at $\rho = 1$ were obtained from the numerical solutions of Equations (9), (10), (11), (9*a*), (10*a*), and (11*a*) for all of the values of N_{Pe} and γ considered. Convergence of the coefficients $f_0'(\rho)$, $f_2'(\rho)$, and $f_4'(\rho)$ was very rapid, and the difference between $f_2'(\rho)$ and $g_2'(\rho)$ was found to be less than 0.5%, indicating that the use of the first approximation for all but the lead term in the series (15) is justified. Therefore solutions to Equations (10*a*) and (11*a*) were for the most part not computed. A partial listing of $f_0'(\rho)$, $f_2'(\rho)$, $f_4'(\rho)$, and $g_0'(\rho)$ and the average Nusselt number computed from Equation (15) is given in Table 1, with the values computed by Yuge (*23*), who considered a single sphere in an infinite fluid medium, as a comparison. A more complete tabulation of these values and of the functions $f_0(\rho)$, $f_2(\rho)$, etc. is found in reference *19*.

By replacing the temperature variable t by a concentration variable c, the thermal diffusivity α by the mass diffusivity D, and the Nusselt number by the Sherwood number one can apply these solutions to mass transfer as

TABLE 1. COMPUTED VALUES OF $f_0'(1)$, $f_2'(1)$, $f_4'(1)$, $g_0'(1)$, AND $(N_{Nu})_{avg}$ AS A FUNCTION OF N_{Pe} AND ϵ

Peclet No.		$\epsilon = 1.0$ Results of Yuge (*24*)	$\epsilon = 0.992$ $\gamma = 0.200$	$\epsilon = 0.963$ $\gamma = 0.333$	$\epsilon = 0.875$ $\gamma = 0.500$	$\epsilon = 0.637$ $\gamma = 0.714$	$\epsilon = 0.488$ $\gamma = 0.800$	$\epsilon = 0.422$ $\gamma = 0.833$
0.3	$f_0'(1)$	1.1807	1.3173	1.5440	2.0300	3.5211	5.0188	—
	$f_2'(1)$	−0.0348	−0.0279	−0.0203	−0.0145	−0.0104	−0.0093	
	$f_4'(1)$	0.0002	0.0012	0.0013	0.0011	0.0008	0.008	
	$g_0'(1)$	1.0939	1.2849	1.5321	2.0265	3.5204	5.0185	
	$(N_{Nu})_{avg}$	2.00	2.44	2.98	4.00	7.00	10.0	
1.0	$f_0'(1)$	1.3557	1.4545	1.6419	2.0989	3.5702	5.0626	6.0600
	$f_2'(1)$	−0.0589	−0.0633	−0.0558	−0.0445	−0.0338	−0.0306	−0.0295
	$f_4'(1)$	0.0000	0.0006	0.0009	0.0026	0.0025	0.0024	0.0023
	$g_0'(1)$	1.2733	1.3934	1.6113	2.0884	3.5680	5.0617	6.0595
	$(N_{Nu})_{avg}$	2.20	2.43	2.95	3.99	7.01	10.01	11.96
5.0	$f_0'(1)$	—	1.9324	2.0833	2.4599	3.8448	5.3096	—
	$f_2'(1)$		−0.1267	−0.1406	−0.1513	−0.1462	−0.1405	
	$f_4'(1)$		−0.0002	0.0006	0.0023	0.0070	0.0088	
	$g_0'(1)$		1.8737	2.0324	2.4296	3.8354	5.3060	
	$(N_{Nu})_{avg}$		3.00	3.26	4.03	7.00	10.03	
10.0	$f_0'(1)$	2.0842	2.2656	2.4503	2.8347	4.1723	5.6125	6.5906
	$f_2'(1)$	−0.1431	−0.1629	−0.1828	−0.2162	−0.2495	−0.2544	−0.2551
	$f_4'(1)$	−0.0003	−0.0003	−0.0004	0.0005	0.0072	0.114	0.0113
	$g_0'(1)$	2.0301	2.2164	2.4052	2.8000	4.1570	5.6057	6.5864
	$(N_{Nu})_{avg}$	3.20	3.47	3.75	4.34	7.04	10.03	11.98
50.0	$f_0'(1)$	—	3.4471	3.7733	4.4149	6.1223	7.6927	8.6843
	$f_2'(1)$		−0.2866	−0.3205	−0.3883	−0.5739	−0.7151	−0.7806
	$f_4'(1)$		−0.0006	−0.0006	−0.0007	0.0002	0.0051	0.0063
	$g_0'(1)$		3.4164	3.7454	4.3912	6.1223	7.6777	8.6745
	$(N_{Nu})_{avg}$		5.13	5.59	6.48	9.22	11.30	12.94
100.0	$f_0'(1)$	—	—	—	—	7.6296	9.5513	10.6815
	$f_2'(1)$					−0.7338	−0.9494	−1.0526
	$f_4'(1)$					0.0234	0.0170	0.0062
	$g_0'(1)$					7.6161	9.5405	10.6720
	$(N_{Nu})_{avg}$					11.56	13.97	15.34

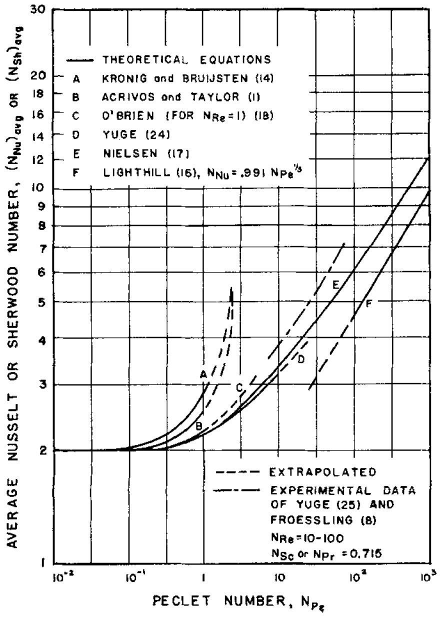

Fig. 1. Theoretical equations for heat and mass transfer from a single sphere at low Reynolds numbers.

well as to heat transfer. One can also consider the effect of a chemical reaction occurring at the surface of the particle. For example if a simple first-order reaction with no net increase in the number of moles is assumed, then

$$D\left(\frac{dc}{dr}\right)_{r=a} = k_R\,(c)_{r=a} \qquad (16)$$

where k_R is the heterogeneous first-order reaction rate constant. If one now defines $\psi' = c/C_o$ as a reduced concentration coordinate [this does not in any way affect Equation (1*a*)], then in terms of dimensionless variables

$$\left(\frac{d\psi'}{d\rho}\right)_{\rho=1} = R(\psi')_{\rho=1} \qquad (16a)$$

where R = Damköhler's group = $(k_R a)/(D)$.

Since the solution of Equation (1*a*) has been approximated by a series of the form

$$\psi' = f_0(\rho) + f_2(\rho)\theta^2 + f_4(\rho)\theta^4 + \ldots. \qquad (7)$$

the boundary condition given by Equation (16*a*) becomes

$$f_0'(\rho) = R\,f_0(\rho);\, f_2'(\rho) = R\,f_2(\rho);\, f_4'(\rho) = R\,f_4(\rho)$$
$$g_0'(\rho) = R\,g_0(\rho)\,\ldots\ldots \text{at } \rho = 1 \qquad (16b)$$

Solutions to Equations (9), (10), (11), (9*a*), etc. using equations (16*b*) and the second boundary condition that

$$f_0(\rho) = 1, f_2(\rho) = f_4(\rho) = 0 \text{ at } \rho = 1/\gamma \qquad (17)$$

allows one to obtain the concentration at the surface of the particle.

Analysis of Results—Single Sphere

Since the solution to the energy Equation (1*a*) is based on the method of successive approximations suggested by Yuge (*24*) in his theoretical study of heat transfer from a single sphere to a fluid in Stokes' flow, it is appropriate to examine his results in detail. Yuge's theory agrees quite well (within 2%) with the results of Nielsen (*17*), who solved the energy equation numerically using a relaxation technique, but disagrees with a recent solution presented by Acrivos and Taylor (*1*) by about 15% at N_{Pe} = 1.0. Although Acrivos' singular perturbation expansion seems quite rigorous at very low N_{Pe}, it cannot be determined at what value of N_{Pe} it will break down. O'Brien (*18*), like Acrivos and Taylor, also used the method of singular perturbation expansions but employed the Oseen approximation rather than the Stokes solution in the outer expansion and found that N_{Nu} depends on N_{Re} as well as on N_{Pe}. O'Brien's solution agrees with Acrivos and Taylor's only at very low Reynolds numbers ($N_{Re} \leqq 0.03$). The solutions of Yuge and Nielsen are also found to be in good agreement with the asymptotic development for high Peclet numbers presented by Lighthill (*16*). For comparison all of the theoretical correlations have been plotted in Figure 1.

Experimental verification of Yuge's and other theoretical solutions to the single sphere problem has been limited owing to the difficulty of obtaining accurate heat and mass transfer data at very low Reynolds numbers because of natural convection effects. For Reynolds numbers of 100 or less experimental data have been reported by Allander (*2*), Ranz and Marshall (*21*), Froessling (*8*), and Yuge (*25*). The experimental correlations of the latter two authors in the N_{Re} range of 10 to 100 are plotted in Figure 1; unfortunately no data in the low Peclet number range of 0.5 to 5.0 are available. Lastly it might be significant to mention that in presenting a general correlation of the Nusselt or Sherwood number with Peclet number for the entire range of N_{Pe} Friedlander (*6*) combined the Yuge results for $N_{Pe} \leqq 10$ with his own boundary-layer theory results for $N_{Pe} > 100$.

Analysis of Results—Free Surface Model

Figure 2 is a plot of the average Nusselt or Sherwood number vs. the fractional void volume of a multiparticle system with the Peclet number as a parameter. The void volume ϵ is directly related to the quantity γ by the geometry of the free surface model ($\epsilon = 1 - \gamma^3$). The plot shows that the average Nusselt number increases sharply as the bed becomes more concentrated (low ϵ) for all values of the Peclet number. As the bed fractional void volume approaches unity (a single particle in an infinite fluid), the Nusselt number increases with Peclet number at all values of N_{Pe}; as the bed becomes more concentrated, the effect of N_{Pe} decreases, and at a porosity $\epsilon <$ 0.7 the Nusselt number becomes independent of the Peclet number in the low *Pe* range (N_{Pe} = 0.3 to N_{Pe} = 10). The reason for this behavior is that although the Nusselt

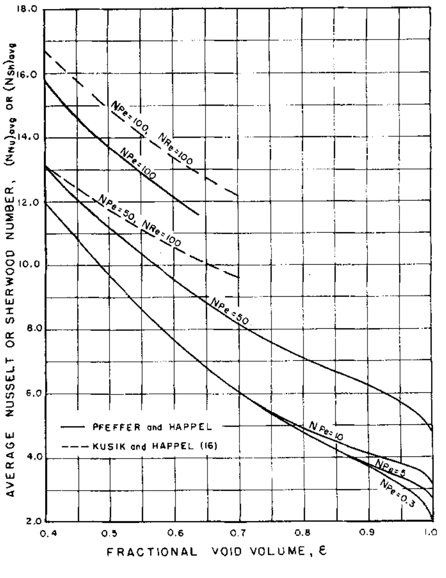

Fig. 2. Average Nusselt number vs. voidage.

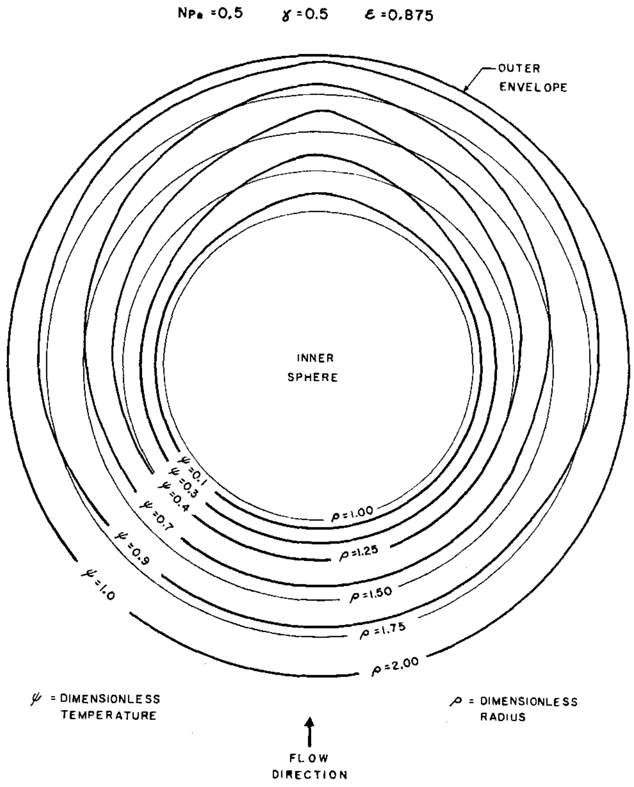

Fig. 3. Typical temperature or concentration profile in a fluid surrounding a particle.

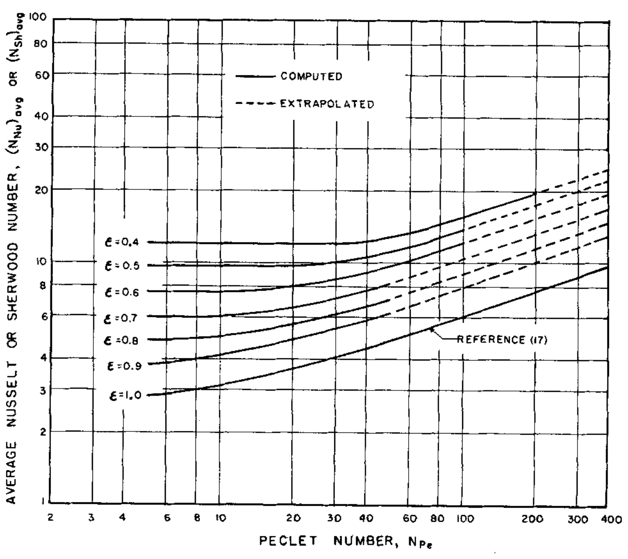

Fig. 4. Average Nusselt number vs. Peclet number.

number at the forward stagnation point ($\theta = 0$) for a given porosity was always found to increase with Peclet number, the Nusselt number behind the sphere was found to decrease as the Peclet number is increased. This seems to be caused by a decrease in the temperature gradient at the rear of the particle due to a general increase in fluid temperature as the cold fluid flows past the hot particle at higher Peclet numbers. An indication of the fluid temperature profile is illustrated by Figure 3. It is interesting to point out that a symmetrical fluid flow pattern gives rise to an unsymmetrical temperature pattern around the particle.

A cross plot of Figure 2 showing the Nusselt number as a function of the Peclet number with voidage as a parameter is given in Figure 4. At high Peclet numbers the Nusselt number appears to become a simple exponential function of the Peclet number which can be represented by the equation

$$(N_{Nu})_{\text{avg}} = B_\epsilon \, Pe^{1/3} \tag{18}$$

where B_ϵ is a constant depending on the value of ϵ. Equation (18) is identical in form to the asymptotic solution for high Peclet numbers given by Lighthill (*16*) for the single sphere problem.

Since almost all of the experimental heat and mass transfer data for packed beds are correlated in the literature by plotting a dimensionless j factor vs. a dimensionless Reynolds number, one should replot the results of Figure 2 in terms of these parameters. Figure 5 is a typical plot of j against N_{Re} at $\epsilon = 0.488$ (a good representative void fraction for a packed bed) for four different values of the Prandtl (or Schmidt) number. The plot clearly indicates that j is not independent of the Prandtl number when the Reynolds or Peclet number is small. At very low Reynolds numbers the curves in Figure 5 are straight lines with slope $= -1.0$. As the Reynolds number increases, the slope of the curves deviate from unity, the deviation beginning at smaller Reynolds numbers as the Prandtl number increases. If the curves for $N_{Pr} = 10$, 100, and 1,000 are extrapolated to higher Reynolds numbers, they all merge into a single straight line of slope $= -2/3$ at a value of $N_{Pe} = N_{Re} \times N_{Pr}$ of about 70. This indicates that the j factor does become independent of the Prandtl number at high Peclet numbers and can be represented by the equation

$$j = B_\epsilon \, N_{Re}^{-2/3} \tag{18a}$$

Since j is defined by $j = (N_{Nu})/(N_{Re} N_{Pr}^{1/3})$, Equation (18*a*) follows directly from Equation (18). From Figure 5, B_ϵ is found to be equal to 3.0 when $\epsilon = 0.488$. This result also agrees with a recent boundary-layer solution by Pfeffer (*20*), who also found that at high Peclet numbers j is independent of N_{Pr} and is a function of $N_{Re}^{-2/3}$.

Similar results are obtained upon plotting j vs. N_{Re} for larger values of ϵ. The curves are simply shifted downward; that is j becomes smaller at a given value of N_{Re} and approaches the limiting value for a single particle as

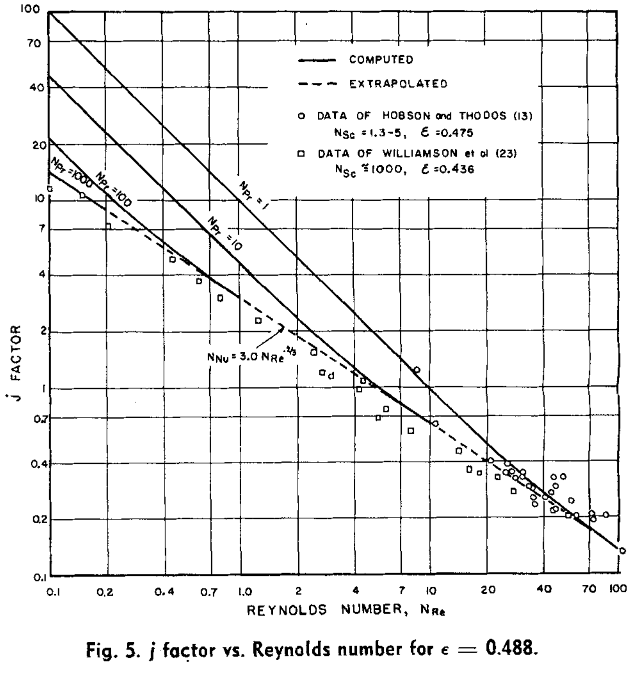

Fig. 5. j factor vs. Reynolds number for $\epsilon = 0.488$.

$\epsilon \to 1.0$. This is illustrated by Figure 6, which is a plot of j vs. N_{Re} for different values of ϵ at N_{Pr} (or N_{Sc}) = 1.0. If N_{Pr} is taken as 1.0 (gas systems), one can obtain j factors from Figure 6 for Reynolds numbers as high as 100. The extension of theoretical results which are based on an analytical treatment involving viscous forces alone to such high Reynolds numbers can be justified only by the fact that the results agree with experimental data, and that since this paper considers flow in packed beds (ϵ = 0.4 to 0.6) the separation phenomenon is much less pronounced than for flow at higher porosities.

The experimental data of different investigators for heat and mass transfer in packed and fluidized beds (*3, 4, 5, 9, 10, 13, 22, 23*) are not very consistent, especially at low Reynolds numbers. Nevertheless the theoretical curve of j vs. N_{Re} at a $N_{Pr} = N_{Sc} = 1.0$ at $\epsilon = 0.5$ (Figure 6), which can be considered to be an adequate representation of gas-phase mass transfer, agrees identically with the experimental correlation presented by Hobson and Thodos (*13*), although their correlation was given as independent of Schmidt number. On the other hand Dryden, Strang, and Withrow (*5*), like Hobson and Thodos (*13*), also found that a plot of j vs. N_{Re} results in a straight line of slope equal to minus unity at very low N_{Re}; they obtained two different curves for the two different solid-liquid systems studied, although the two curves appeared to converge as the Reynolds number was increased. The conclusion that j is a function of Schmidt number as well as Reynolds number in the low Reynolds number range was also obtained by Thoenes and Kramers (*22*), who found that j is highest for gas-phase mass transfer and lowest for high Schmidt number liquid-phase mass transfer. The gas-phase data of Hobson and Thodos (*13*) (N_{Sc} = 1.3-5, ϵ = 0.475) and the recent liquid-phase data of Williamson et al. (*23*) ($N_{Sc} \cong 1000$, $\epsilon \cong 0.43$) are plotted in Figure 5 and show close agreement with the theoretical curves.

Although not plotted because of the many different voidages involved, the pertinent liquid-phase data of Gaffney and Drew (*9*) and Dryden, Strang, and Withrow (*5*), the gas-phase data of Chu et al. (*4*), and the extrapolated data of Gamson et al. (*10*) also agree quite well with the theoretical results. Unfortunately data are not available in the very low Reynolds number, low Peclet number range so that data at higher Reynolds numbers had to be used in an attempt to verify the theory.

Last, a comparison of the authors' results with the theoretical correlation developed by Kusik and Happel (*16*)

$$N_{Sh}\, N_{Re}^{-1/2}\, N_{Sc}^{-1/3} = 0.93\, [\epsilon - 0.75\,(1-\epsilon)\,(\epsilon - 0.2)]^{-1/2} \qquad (19)$$

which was obtained by using a combination of the free surface model and boundary-layer theory, shows fairly good agreement, especially at the lower porosities (see Figure 2). Deviations at the higher porosities are expected since the Kusik and Happel correlation applies to $N_{Re} >$ 100, whereas the creeping motion velocity distribution which was used here cannot be expected to apply at these high Reynolds numbers when the particle concentration is small owing to separation effects.

Free Surface Model with Surface Chemical Reaction

To apply the authors' model to diffusion with surface chemical reaction a simple first-order surface reaction, $A \to B$ was considered. The pertinent differential equations were solved for a bed porosity $\epsilon = 0.488$ ($\gamma = 0.8$) for five different values of R at four different N_{Pe} with the boundary conditions given by Equations (16*b*) and (17). The average surface concentration was then computed by integrating the local concentration over the surface of the sphere. The results are plotted in Figure 7 and indicate that the average surface concentration $\psi_i' = \left(\frac{c}{C_o}\right)_{\rho=1}$ is a function of R but is independent of Peclet number until the Peclet number is raised above 10. This agrees with previous results which have shown that the average Sherwood number also does not change with N_{Pe} at $N_{Pe} \leqq 10$ at this high particle concentration. As the value of R becomes very large, the rate of reaction becomes very rapid and the surface concentration approaches zero and diffusion is the controlling resistance. As R approaches zero, the surface concentration approaches C_o ($\psi' \to 1.0$) indicating that the resistance due to diffusion is negligible compared with that due to the reaction. The average surface concentration could also have been obtained by assuming that the average Sherwood number remains constant even though the local surface concentration and

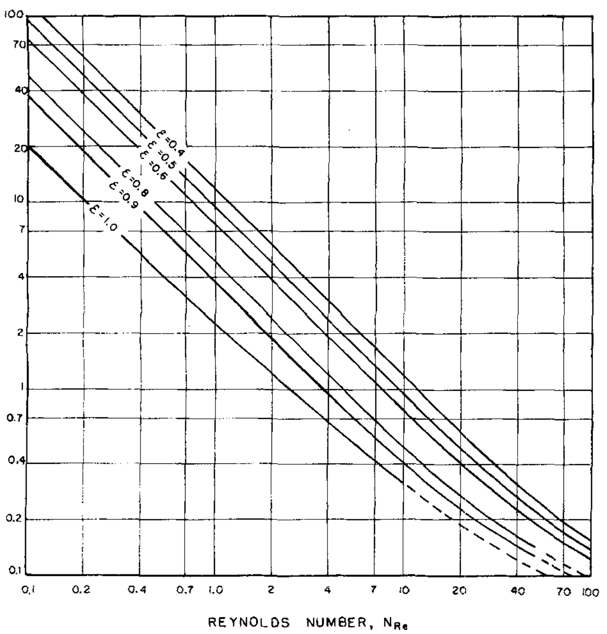

Fig. 6. j factor vs. Reynolds number for N_{Pr} or N_{Sc} = 1.0.

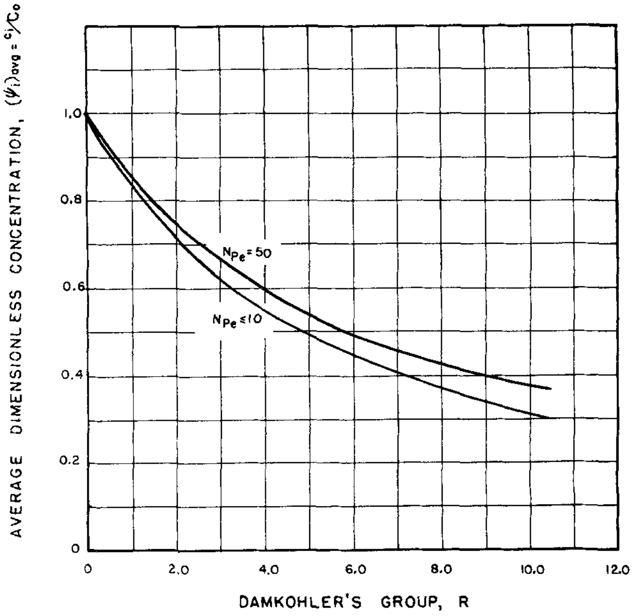

Fig. 7. Surface concentration with first-order chemical reaction in a packed bed, ϵ = 0.488.

therefore the local transfer rate vary over the surface of the particle. If one makes this assumption then

$$\frac{(\psi_i')_{avg}}{1-(\psi_i')_{avg}} = \frac{(N_{Sh})_{avg}}{2R} \qquad (20)$$

A comparison between the values of $(\psi_i')_{avg}$ obtained from Equation (20) with those computed from the solutions of the differential equations shows an average deviation of less than 2%. Hence the use of this approximation at these low Peclet numbers seems justified, and the authors' model can therefore be applied to more complex surface chemical reactions with very little added difficulty.

CONCLUSIONS

A rapidly converging solution to the energy equation coupled with the free surface model is obtained if the fluid temperature distribution is expanded in even powered terms of the spherical angle as suggested by Yuge. No more than the first three terms of the first approximation and the lead term of the second approximation are required to give a solution numerically accurate to within 3%. A comparison of the theoretical solutions at different Peclet numbers and bed porosities to some of the experimental packed bed data shows fairly close agreement and also indicates that the *j* factor is not independent of the Schmidt number at low Peclet number flow. Extension of the model to include a simple surface chemical reaction coupled with diffusion was also successful.

ACKNOWLEDGMENT

This research was supported by a grant from the Petroleum Research Fund administered by the American Chemical Society. Grateful acknowledgment is hereby made to the donors of the fund. The authors also wish to thank Howard Brenner and C. L. Kusik for their valuable comments and suggestions.

NOTATION

a = radius of inner sphere, ft.
b = radius of outer sphere, ft.
c = molar concentration, lb. moles/cu. ft.
C_p = specific heat of fluid, B.t.u./(lb.) (°F.)
d = diameter of inner sphere or of a particle in a multiparticle system, ft.
D = mass diffusivity, sq. ft./hr.
A, B, C, D = constants defined by Equation (6), dimensionless
$f_0(\rho), f_2(\rho), f_4(\rho)$ = functions of ρ defined by Equation (7), dimensionless
$g_0(\rho), g_2(\rho), g_4(\rho)$ = functions of ρ defined by Equation (12), dimensionless
h = convective heat transfer coefficients, B.t.u./(hr.) (sq. ft./°F.)
j = Colburn j factor $= \dfrac{N_{Sh}}{N_{Re}\,N_{Sc}}\,(N_{Sc})^{2/3} = \dfrac{N_{Nu}}{N_{Re}\,N_{Pr}}\,(N_{Pr})^{2/3}$, dimensionless
K_c = convective mass transfer coefficient, ft./hr. or moles/(hr.) (sq. ft./atm.)
k = thermal conductivity of fluid, B.t.u./(hr.) (ft./°F.)
k_R = first-order surface reaction rate constant, ft./hr.
N_{Nu} = local Nusselt number $= hd/k$, dimensionless
$(N_{Nu})_{avg}$ = average Nusselt number, dimensionless
N_{Pr} = Prandtl number $= C_p\,\mu/k$, dimensionless
N_{Pe} = Peclet number $= N_{Re} \times N_{Pr}$ or $N_{Re} \times N_{Sc}$, dimensionless
r = radial direction in a spherical coordinate, ft.
N_{Re} = Reynolds number $= dV\,\rho'/\mu$, dimensionless
R = Damköhler group $= k_R\,a/D$, dimensionless
N_{Sh} = local Sherwood number $= K_c\,d/D$, dimensionless
$(N_{Sh})_{avg}$ = average Sherwood number, dimensionless
N_{Sc} = Schmidt number $= \mu/\rho' D$, dimensionless
t = temperature, °F.
V = superficial velocity of flow in a packed bed or free stream velocity, ft./hr.
v_r = fluid velocity component in the radial direction, ft./hr.
v_θ = fluid velocity component in the θ direction, ft./hr.

Greek Letters

α = thermal diffusivity, sq. ft./hr.
γ = ratio of inner sphere to outer sphere radii $= a/b$, dimensionless
ϵ = fractional void volume, dimensionless
ρ = dimensionless radius $= r/a$, dimensionless
ρ' = density of fluid, lb./cu. ft.
θ = spherical angle in a spherical coordinate system, rad.
μ = viscosity of fluid, lb./(ft.) (hr.)
ψ = dimensionless temperature or concentration $\dfrac{T_1 - t}{T_1 - T_o}$ or $\dfrac{C_1 - c}{C_1 - C_o}$, dimensionless
ψ' = dimensionless concentration c/C_o, dimensionless
$\tau_{r\theta}$ = shearing stress, lb./sq. ft.

Subscripts

1 or i = at the surface of the inner sphere ($r = a$)
0 = at the surface of the outer sphere ($r = b$)

LITERATURE CITED

1. Acrivos, A., and T. D. Taylor, *Phys. Fluids,* **5,** 387 (1962).
2. Allander, C., *Trans. Royal Inst. Technol. Stockholm,* **70,** (1953).
3. Bar-Ilan, M., and W. Resnick, *Ind. Eng. Chem.,* **49,** 313 (1957).
4. Chu, J. D., J. Kalil, and W. A. Wetteroth, *Chem. Eng. Progr.,* **49,** 141 (1953).
5. Dryden, C. E., D. A. Strang, and A. E. Withrow, *ibid.,* p. 191.
6. Friedlander, S. R., *A.I.Ch.E. Journal,* **3,** 43 (1957); **7,** 348 (1961).
7. Frisch, H. L., *J. Chem. Phys.,* **22,** 123 (1954).
8. Froessling, N., *Beitrag Geophys.,* **52,** 170 (1938).
9. Gaffney, B. W., and T. B. Drew, *Ind. Eng. Chem.,* **42,** 1120 (1950).
10. Gamson, B. W., George Thodos, and P. A. Hougen, *Trans. Am. Inst. Chem. Engrs.,* **39,** 1 (1945).
11. Happel, John, *A.I.Ch.E. Journal,* **4,** 197 (1958).
12. *Ibid.,* **5,** 174 (1959).
13. Hobson, M., and George Thodos, *Chem. Eng. Progr.,* **45,** 517 (1949); **47,** 370 (1951).
14. Kronig, R., and J. Bruijsten, *Appl. Sci. Res.,* **2,** 439 (1951).
15. Kusik, C. L., and John Happel, *Ind. Eng. Chem. Fundamentals,* **1,** 163 (1960).
16. Lighthill, M. J., *Proc. Royal Soc.,* **A202,** 359 (1950).
17. Nielsen, A. E., *J. Phys. Chem.,* **65,** 46 (1961).
18. O'Brien, Vivian, Applied Physics Laboratory, The Johns Hopkins Univ., Silver Springs, Md., report on "Slow Forced Convection with Moving Drops," supported by the Dept. of the Navy under Contract No. 62,0604c (1962).
19. Pfeffer, Robert, Ph.D. thesis, New York University, New York, New York (1962).
20. ———, paper in progress (1963).
21. Ranz, W. E., and W. R. Marshall, *Chem. Eng. Progr.,* **48,** 141 (1952).
22. Thoenes, D., and H. Kramers, *Chem. Eng. Sci.,* **8,** 271 (1958).
23. Williamson, J. E., K. E. Bazaire, and C. J. Geankoplis, *Ind. Eng. Chem. Fundamentals,* **2,** 126 (1963.)
24. Yuge, T., *Rept. Inst. High Speed Mechanics of Tohoku Univ.,* **6,** 143 (1956).
25. ———, *Trans. Am. Soc. Mech. Engrs.,* **82,** 214 (1960).

Manuscript received March 11, 1963; revision received February 20, 1964; paper accepted February 21, 1964. Paper presented at A.I.Ch.E. Buffalo meeting.